

# **Adrenaline stimulates glucagon secretion by Tpc2-dependent $\text{Ca}^{2+}$ mobilization from acidic stores in pancreatic $\alpha$ -cells**

Alexander Hamilton<sup>1</sup>, Quan Zhang<sup>1</sup>, Albert Salehi<sup>2</sup>, Mara Willems<sup>1</sup>, Jakob G. Knudsen<sup>1</sup>, Sam Stephen<sup>1</sup>, Anna K. Ringgaard<sup>3,4</sup>, Caroline E. Chapman<sup>1</sup>, Alejandro Gonzalez-Alvarez<sup>1</sup>, Nicoletta C. Surdo<sup>5</sup>, Manuela Zaccolo<sup>5</sup>, Davide Basco<sup>6</sup>, Paul R.V. Johnson<sup>1,7</sup>, Reshma Ramracheya<sup>1</sup>, Guy A. Rutter<sup>8</sup>, Antony Galione<sup>9</sup>, Patrik Rorsman<sup>1,2,7</sup> and Andrei I. Tarasov<sup>1,7\*</sup>

<sup>1</sup>Oxford Centre for Diabetes, Endocrinology and Metabolism, University of Oxford. Churchill Hospital, Headington, OX3 7LE, Oxford, UK

<sup>2</sup>Institute of Neuroscience of Physiology, Department of Physiology, Metabolic Research Unit, University of Göteborg, Göteborg, Sweden

<sup>3</sup>Novo Nordisk A/S, Diabetes Research, Department of Stem Cell Biology, Novo Nordisk Park, 2760, Måløv, Denmark

<sup>4</sup>University of Copenhagen, Department of Biomedical Sciences, Blegdamsvej 3B, 2200, Copenhagen, Denmark

<sup>5</sup>Department of Physiology, Anatomy and Genetics, University of Oxford, Oxford, UK

<sup>6</sup>Center for Integrative Genomics, Université de Lausanne, Lausanne, Switzerland

<sup>7</sup>Oxford National Institute for Health Research, Biomedical Research Centre, Oxford, UK

<sup>8</sup>Section of Cell Biology and Functional Genomics, Department of Medicine, Imperial College London, London, UK

<sup>9</sup>Department of Pharmacology, University of Oxford, Oxford, UK

\*Corresponding author: University of Oxford, OCDEM, Churchill Hospital, OX3 7LE Oxford UK

Tel +441865857071 Email: [andrei.tarasov@ocdem.ox.ac.uk](mailto:andrei.tarasov@ocdem.ox.ac.uk)

List of abbreviations: NAADP, nicotinic acid adenine dinucleotide phosphate; PKA, protein kinase A; EPAC2, exchange protein directly activated by cAMP, isoform 2; cAMP, cyclic adenosine monophosphate; TPC, two-pore channel; pAUC, partial area under the curve; IP<sub>3</sub>, inositol trisphosphate; CICR, Ca<sup>2+</sup>-induced Ca<sup>2+</sup> release; BSA, bovine serum albumin; sER, sarco/endoplasmic reticulum; AKAR-3, A-kinase activity reporter version 3;

Word count: 3,996      Limit: 4,000

Running title: Adrenaline controls Ca<sup>2+</sup> release in  $\alpha$ -cells

## Abstract

Adrenaline is a powerful stimulus of glucagon secretion. It acts by activation of  $\beta$ -adrenergic receptors but the downstream mechanisms have only been partially elucidated. Here we have examined the effects of adrenaline in mouse and human  $\alpha$ -cells by a combination of electrophysiology, imaging of  $\text{Ca}^{2+}$  and PKA activity and hormone release measurements. We found that stimulation of glucagon secretion correlated with a PKA- and EPAC2-dependent (inhibited by PKI and ESI-05, respectively) elevation of  $[\text{Ca}^{2+}]_i$  in  $\alpha$ -cells, which occurred without stimulation of electrical activity, persisted in the absence of extracellular  $\text{Ca}^{2+}$  but was sensitive to ryanodine, bafilomycin and thapsigargin. Adrenaline also increased  $[\text{Ca}^{2+}]_i$  in  $\alpha$ -cells in human islets. Genetic or pharmacological inhibition of Tpc2 channel (that mediates  $\text{Ca}^{2+}$  release from acidic intracellular stores) abolished the stimulatory effect of adrenaline on glucagon secretion and reduced the elevation of  $[\text{Ca}^{2+}]_i$ . Furthermore, in Tpc2-deficient islets, ryanodine exerted no additive inhibitory effect. These data suggest that  $\beta$ -adrenergic stimulation of glucagon secretion is controlled by a hierarchy of  $[\text{Ca}^{2+}]_i$  signaling in the  $\alpha$ -cell that is initiated by cAMP-induced Tpc2-dependent  $\text{Ca}^{2+}$  release from the acidic stores and further amplified by  $\text{Ca}^{2+}$ -induced  $\text{Ca}^{2+}$  release from the sarco/endoplasmic reticulum.

## Key words

Pancreatic  $\alpha$ -cells, adrenaline, glucagon, two-pore channels

## Introduction

The ability of the 'fight-or-flight' hormone adrenaline to increase plasma glucose levels by stimulating liver gluconeogenesis is in part mediated by glucagon, the body's principal hyperglycemic hormone (1). Glucagon is secreted by the  $\alpha$ -cells of the pancreas (2). Reduced autonomic stimulation of glucagon secretion may result in hypoglycemia, a serious and potentially fatal complication of diabetes (3). It has been estimated that up to 10% of insulin-treated patients die of hypoglycemia (4). Understanding the mechanism by which adrenaline stimulates glucagon secretion and how it becomes perturbed in diabetic patients is therefore essential.

The mechanism by which adrenaline stimulates glucagon secretion has only partially been elucidated. It is clear, however, that it involves activation of  $\beta$ -adrenergic receptors (5-7), leading to elevated intracellular cAMP ( $[cAMP]_i$ ), and culminates in elevation of the cytoplasmic free  $Ca^{2+}$  concentration ( $[Ca^{2+}]_i$ ) with resultant  $Ca^{2+}$ -dependent stimulation of glucagon secretion (6;8;9). However, our understanding of the spatiotemporal inter-relationship between different intracellular  $Ca^{2+}$  stores involved in the  $\alpha$ -cell adrenaline signaling remains patchy.

Here we have explored how adrenaline, via activation of  $\beta$ -adrenergic receptors, triggers glucagon release by a combination of glucagon secretion measurements, electrophysiology and imaging of cytoplasmic  $Ca^{2+}$ , cAMP and PKA activity in  $\alpha$ -cells in intact mouse pancreatic islets. We have extended the measurements to human islets and also tested how the responsiveness to adrenaline is affected when islets are cultured under hyperglycemic conditions to establish if and how this regulation becomes impaired in diabetes. Our data indicate that  $Ca^{2+}$  release from acidic (lysosomal) stores plays a critical and unexpected role in adrenaline-induced glucagon secretion.

## Research Design and Methods

### Chemicals

The following substances were used (source given in parentheses): the L-type  $\text{Ca}^{2+}$  channel blocker isradipine and the P/Q  $\text{Ca}^{2+}$  channel blocker  $\omega$ -agatoxin (Alomone Labs; Jerusalem, Israel); the  $\alpha_1$ -antagonist prazosin (Abcam, Cambridge, UK); the membrane-permeable PKA inhibitor myr-PKI, the  $\text{IP}_3$  receptor inhibitor Xestospongine C, the NAADP antagonist Ned-19, the V-ATPase inhibitor bafilomycin, the sER ATPase inhibitor thapsigargin and noradrenaline (Tocris Bioscience, Bristol, UK); the EPAC2 inhibitor ESI-05 (BioLog, Bremen, Germany); the insulin receptor antagonist (S961, Novo-Nordisk, Denmark). All other compounds were obtained from Sigma-Aldrich (Dorset, UK).

### Solutions

The extracellular solution (EC1) used for imaging and current-clamp electrophysiology (Figure 2c) experiments contained (mM) 140 NaCl, 4.6 KCl, 2.6  $\text{CaCl}_2$ , 1.2  $\text{MgCl}_2$ , 1  $\text{NaH}_2\text{PO}_4$ , 5  $\text{NaHCO}_3$ , 10 HEPES (pH 7.4, with NaOH). The pipette solution (IC1) consisted of (mM) 76  $\text{K}_2\text{SO}_4$ , 10 NaCl, 10 KCl, 1  $\text{MgCl}_2$ , 5 HEPES (pH 7.35 with KOH). The extracellular solution (EC2) for recordings of the depolarization-induced exocytosis (Figure 3c,d) contained (mM) 118 NaCl, 5.6 KCl, 2.6  $\text{CaCl}_2$ , 1.2  $\text{MgCl}_2$ , 5 HEPES, 20 TEA-Cl and 6 glucose (pH 7.4 with NaOH). In the latter experiments, the pipette-filling medium (IC2) consisted of (mM) 76  $\text{Cs}_2\text{SO}_4$ , 10 NaCl, 10 KCl, 1  $\text{MgCl}_2$ , 5 HEPES (pH 7.35 with CsOH).

### Animals, islet isolation and culture

NMRI mice (Charles River) were used throughout the study except for the experiments involving the genetic manipulation of TPC1 and 2 (Figure 5). *Tpcn1*<sup>-/-</sup> and *Tpcn2*<sup>-/-</sup> mice were developed on C57Bl6/N background as described (10). *Cd38*<sup>-/-</sup> mice were developed on C57Bl6/J background (11). Age- and sex-matched C57Bl6/N and C57Bl6/J wild-type animals were used as controls. Mice were kept in a conventional vivarium with a 12-hour-dark/12-hour-light cycle with free access to food and water and were killed by cervical dislocation. All experiments were conducted in accordance with the United Kingdom Animals (Scientific Procedures) Act (1986) and the University of Oxford ethical guidelines.

Pancreatic islets were isolated from mice by injecting collagenase solution into the bile duct, with subsequent digestion of the connective and exocrine pancreatic tissue.

Human pancreatic islets were isolated in the Oxford Diabetes Research & Wellness Foundation Human Islet Isolation Facility according to published protocols (12;13).

Unless otherwise stated, experiments were performed on acutely isolated islets. For experiments aiming to emulate chronic hyperglycemia, islets were cultured for 48h in RPMI medium containing 30mM or the standard 11mM glucose, supplemented with 10% FBS, 100IU/mL penicillin and 100µg/mL streptomycin (all reagents from Life Technologies, Paisley, UK). Recombinant sensors were delivered via adenoviral (GCamp6, AKAR3) or BacMam (cADDiS) vectors at  $10^5$  infectious units per islet, followed by 24-36h culturing at 11 mM glucose (as above) to express the sensors.

### **Imaging of $[Ca^{2+}]_i$ , cAMP and PKA activity in islet cells**

Time-lapse imaging of  $[Ca^{2+}]_i$  in intact freshly isolated mouse islets was performed on an inverted Zeiss AxioVert 200 microscope equipped with Zeiss 510-META laser confocal scanning system. Prior to  $Ca^{2+}$  imaging, mouse islets were loaded with 6µM Fluo-4 at room temperature or 10 µM Fluo4FF (Molecular Probes) at +37°C for 90 min. Both dyes were excited at 488nm and emission was collected at 530nm, using 512x512 frame scanning mode with the pixel dwell time of 6µs (image frequency: 0.25Hz). Time-lapse imaging of  $[Ca^{2+}]_i$  in groups of mouse islets was done on a Axiozoom.V16 microscope (0.1Hz) using Gcamp6f (14).

PKA activity was reported in pancreatic islet cells using recombinant FRET probe AKAR3 (15). AKAR3 CFP fluorescence was excited at 458nm using an Axiozoom.V16 microscope, which has been shown previously to excite CFP selectively (16); the emitted light was collected at 485nm (CFP) and 515nm (YFP) (image frequency: 0.0Hz). Time-lapse imaging of  $[cAMP]_i$  was performed using recombinant Green Downward cADDiS sensor (Montana Molecular, Bozeman, Montana, U.S.A.). The cADDiS fluorescence was excited at 485nm and the emission recorded at 515nm using an Axiozoom.V16 microscope. PKA and cAMP were imaged at a frequency of 16 mHz.

All imaging at 34°C was performed using an open chamber. The bath solution containing various stimuli was perfused continuously at a rate of 200  $\mu$ l/min. In experiments involving PKI, ESI-05, ryanodine, xestospongin C, Ned-19 thapsigargin and the  $\text{Ca}^{2+}$  channel blockers  $\omega$ -agatoxin and isradipine, cells were preincubated in the solution of the respective agent for 90min. For the bafilomycin experiments, the pre-incubation time was 20 min. By pre-incubating the islets in the agonist/antagonist solutions we aimed to reach the saturation of the effect by the start of the recording.  $\alpha$ -Cells were identified as those exhibiting a response to 1mM glutamate (Figure 1c-e) (17) and/or adrenaline (known to inhibit secretion of both insulin and somatostatin) (18).

Images were acquired using ZenBlack or ZenBlue software (Carl Zeiss).

### Hormone release measurements

Batches of 10–20 size-matched freshly isolated mouse islets were pre-incubated in 1ml of Krebs-Ringer buffer containing 1 mM glucose and 0.2% BSA for 30min at 37°C, followed by a 1-h test incubation in 1ml of the same medium supplemented as indicated. Glucagon was determined by RIA RIA (Eurodiagnostica, Malmo, Sweden) (19). The experiments on the *Tpcn1*, *Tpcn2* or *Cd38* knockout mice (Figure 5) and control mice were assayed using the MSD glucagon assay (Rockville, MD, USA).

### Electrophysiology

The electrophysiological measurements were performed on  $\alpha$ -cells within freshly isolated intact islets (from NMRI or C57Bl/6 mice), using an EPC-10 patch-clamp amplifier (HEKA Electronics, Lambrecht/Pfalz, Germany) and Pulse software. All electrophysiological experiments were performed at 34°C.  $\alpha$ -Cells were identified as those active at low (3 mM) glucose and were differentiated from  $\delta$ -cells (some of which fire action potentials, albeit at low frequency at this glucose concentration) by the distinct appearance of action potentials (Figure S2a). For the membrane potential recordings (Figure 2c), the perforated patch configuration was used as described previously (20) using solutions IC1 and EC1. Exocytosis was measured as increases in membrane capacitance in  $\alpha$ -cells in intact islets as described previously using the standard whole-cell configuration and IC2 and EC2.

## Data analysis

Image sequences were analyzed (registration, background subtraction, ROI intensity vs time analysis,  $F/F_0$  calculation) using open-source FIJI software (<http://fiji.sc/Fiji>). The numerical data was analyzed using IgorPro package (Wavemetrics). To calculate partial areas under the curve (pAUC), the recording was split into 30s intervals, and area under the curve was computed for each individual interval (Figure S1c), using the trapezoidal integration. Numbers of measurements/cells are specified in Figure legends; the experiments on human islets were performed on islets isolated from 3 donors. Statistical analysis was performed using R (21). Data is presented as the mean values  $\pm$  S.E.M. Mann-Whitney U-test or Wilcoxon's paired test were used to compute the significance of difference between independent and dependent samples, respectively. Multiple comparisons within one experiment were performed using Kruskal-Wallis test with Nemenyi post-hoc analysis (independent samples) or Friedman test with Nemenyi post-hoc analysis (dependent samples).

## Results

We tested the effect of adrenaline on glucagon secretion at a glucose concentration that roughly approximates hypoglycemia *in vivo* (3mM) (22) and minimizes the activity of  $\beta$ - and  $\delta$ -cells (see (23) and (Figure S1b)). Adrenaline stimulated glucagon secretion from isolated mouse pancreatic islets by  $3.8 \pm 0.8$ -fold (Figure 1a), in line with previously reported results (5).

Glucagon secretion is a  $\text{Ca}^{2+}$ -dependent process and is stimulated by an elevation of  $[\text{Ca}^{2+}]_i$  (5). We quantified the adrenaline effect on  $[\text{Ca}^{2+}]_i$  in  $\alpha$ -cells within intact islets using time-lapse laser scanning confocal microscopy. At 3mM glucose, <20% of the cells in isolated pancreatic islets from NMRI mice were active and generated  $[\text{Ca}^{2+}]_i$  oscillations (Figure 1b). Of the spontaneously active cells, over 70% responded to glutamate (Movie1) and were thus identified as  $\alpha$ -cells (17;24). In  $\alpha$ -cells thus identified, adrenaline induced a rapid and reversible increase in  $[\text{Ca}^{2+}]_i$  (Figure 1c-e). Similar effects of adrenaline were observed at 1mM glucose (Figure S1a,e).



The majority of the islet cells (>80%) were inactive at 3mM glucose but were stimulated when glucose was elevated to 20mM, as expected for  $\beta$ - or  $\delta$ -cells (Figure 1e). At 3mM glucose, adrenaline did not affect  $[Ca^{2+}]_i$  in any of these cells (Figure S1b) and at 20mM actually reduced  $[Ca^{2+}]_i$  (not shown). Assessed as pAUC (see Research Design and Methods; Figure S1c), responsiveness to adrenaline strongly correlated with spontaneous  $[Ca^{2+}]_i$  oscillations at 3mM glucose (Pearson's  $r=0.78$ ) and responsiveness to glutamate ( $r=0.81$ ) (Figure S1d). Similar responses to adrenaline and glutamate were observed in human islets (Figure 1d,f) and islets of C57Bl/6N mice (Figure 1f). These data make it unlikely that paracrine effects influence the  $[Ca^{2+}]_i$  responses to adrenaline in  $\alpha$ -cells. Indeed, neither addition of exogenous insulin, nor inhibition of insulin receptor with S961 were able to significantly modify the adrenaline signaling in  $\alpha$ -cells (

Figure S5b).

Glucagon-secreting  $\alpha$ -cells are equipped with several types of voltage-gated  $Ca^{2+}$  channels (25). The effect of adrenaline on glucagon secretion was abolished by inhibition of L-type (with isradipine) but not P/Q-type (with  $\omega$ -agatoxin)  $Ca^{2+}$  channels (Figure 2a). The changes in adrenaline-induced  $[Ca^{2+}]_i$  dynamics produced by isradipine and  $\omega$ -agatoxin (Figure 2b) correlated with the effects of these blockers on glucagon secretion (Figure 2b). When isradipine was applied just before adrenaline, the response to adrenaline was attenuated but not abolished (Figure 2b). The effect of adrenaline on  $[Ca^{2+}]_i$  was mimicked by noradrenaline (released by intraislet adrenergic nerve endings (26)) and by the  $\beta$ -adrenergic agonist isoprenaline but abolished by  $\beta$ -antagonist propranolol. By contrast, the  $\alpha_1$ -adrenergic inhibitor prazosin, reported to inhibit the adrenaline-induced  $[Ca^{2+}]_i$  increases in single  $\alpha$ -cells (6), had no detectable effect (Figure 2b). Thus, the effect of adrenaline on  $\alpha$ -cell  $[Ca^{2+}]_i$  dynamics principally reflects activation of  $\beta$ -receptors.

We tested whether the adrenaline-induced increase in  $[Ca^{2+}]_i$  can be attributed to stimulation of  $\alpha$ -cell action potential firing by whole-cell perforated-patch measurements (20). In agreement with the  $[Ca^{2+}]_i$  measurements,  $\alpha$ -cells were electrically active and fired action potentials at a frequency of  $\sim 1$ Hz

when exposed to 3mM glucose. Adrenaline depolarized  $\alpha$ -cells by 3mV, produced a 10mV reduction of spike height (Figure 2c, Figure S2f), increased the duration of the action potential from 4 to 8ms but did not (except for a moderate stimulation during the initial 4s) increase spike frequency (Figure S2f,g). These small effects of adrenaline on  $\alpha$ -cell electrical activity, possibly reflecting transient activation of a depolarizing store-operated membrane conductance following depletion of the sER  $\text{Ca}^{2+}$  stores (27), cannot account for the pronounced and sustained (several minutes) increases in  $[\text{Ca}^{2+}]_i$  (Figure 1e,f). Indeed, neither hyperpolarizing the plasma membrane with  $\text{K}_{\text{ATP}}$  channel opener diazoxide, nor chelating the extracellular  $\text{Ca}^{2+}$  with EGTA prior to the addition of adrenaline diminished its capacity to increase  $[\text{Ca}^{2+}]_i$  in  $\alpha$ -cells (Figure 2b, Figure S2c-e).

$\beta$ -Adrenergic signaling results in the  $\text{G}_s$ -mediated activation of adenylyl cyclase and hence increases the cytosolic concentration of cAMP ( $[\text{cAMP}]_i$ ) (28) (Figure S3 ), which in turn activates the downstream targets PKA and exchange protein directly activated by cAMP (EPAC2). We determined the significance of PKA and EPAC in the regulation of  $[\text{Ca}^{2+}]_i$  and glucagon secretion using the inhibitors myr-PKI (for PKA) and ESI-05 (for EPAC2). Both myr-PKI and ESI-05 inhibited adrenaline-induced glucagon secretion (Figure 3a) and significantly reduced the adrenaline-induced increase in  $[\text{Ca}^{2+}]_i$  (Figure 3b), with ESI-05 exerting a much stronger effect than myr-PKI on glucagon secretion. The finding that EPAC2 and/or PKA, despite having similar effects on  $[\text{Ca}^{2+}]_i$ , differentially affect adrenaline-induced glucagon secretion ( $p < 0.05$ ), suggests that cAMP-dependent activation of EPAC2 may be more tightly linked to exocytosis.

The effects of adrenaline itself on glucagon secretion have previously been examined previously (5). Here we explored the roles of PKA and EPAC2 on the cAMP-dependent stimulation of the late-stage depolarization-evoked exocytosis (monitored as increases in membrane capacitance). Figure 3c shows the increase in  $C_m$  evoked by a 20ms depolarization from -70 to 0mV, in the absence or presence of cAMP in the patch pipette and following inhibition of PKA or EPAC2; this pulse duration is comparable to that of the  $\alpha$ -cell action potential (see Figure 2c). Under control conditions, exocytotic responses

were small ( $<5fF$ ). When cAMP was included in the pipette, exocytosis was stimulated by  $\sim 10$ -fold (Figure 3c). The stimulatory effect of cAMP on depolarization-evoked exocytosis was resistant to PKI but reduced by ESI-05 (Figure 3c,d). Longer depolarizations evoked larger exocytotic responses but the effects of cAMP and the inhibitors were the same (Figure S4 ).

We explored the effect of adrenaline on  $[cAMP]_i$  and its relationship to  $[Ca^{2+}]_i$  further by imaging the activity of cAMP's downstream target PKA using the FRET sensor AKAR3 (15). In most islet cells, the application of adrenaline reduced  $[cAMP]_i$  (Figure S3 ), probably reflecting the effect of  $\alpha_2$ -adrenergic receptors in  $\beta$ - (29) and  $\delta$ -cells (30). However, in a subset of islet cells ( $\sim 10\%$ , corresponding to  $\alpha$ -cells), adrenaline increased  $[cAMP]_i$  (Figure S3 c). These changes in  $[cAMP]_i$  correlated with increased  $\alpha$ -cell- and reduced  $\beta/\delta$ -cell-activity of PKA (Figure 3e). We compared the adrenaline-induced increases in PKA activity in  $\alpha$ -cells to that produced by increasing concentrations of the adenylyl cyclase activator forskolin (Figure 3f-g). Forskolin dose-dependently increased PKA activity and  $[Ca^{2+}]_i$ ; half-maximal effects were observed at  $0.19 \pm 0.05 \mu M$  and  $5.3 \pm 1.5 \mu M$ , respectively. The increase in PKA activity induced by  $5 \mu M$  adrenaline was equivalent to the effect of  $4.2 \pm 1.1 \mu M$  forskolin (Figure 3h), in agreement with the observation that stimulation of glucagon secretion is only seen at micromolar concentrations of adrenaline (5). The observation that the adrenaline-induced increase in  $[Ca^{2+}]_i$  requires high  $[cAMP]_i$  (=high forskolin) is consistent with the involvement of EPAC2 ( $K_d$  for cAMP  $\approx 10^{-5}$  M (31)) and the previous report that the stimulatory effect of adrenaline on glucagon secretion is dramatically reduced in EPAC2 knock-out islets (5).

The findings that adrenaline produces a marked increase in  $[Ca^{2+}]_i$  despite having only a marginal effect on  $\alpha$ -cell electrical activity and that it retains the capacity to stimulate glucagon secretion in the absence of extracellular  $Ca^{2+}$  and in the presence of a high concentration of the  $K_{ATP}$  channel activator diazoxide (to suppress electrical activity (20)) suggest that it, via activation of  $\beta$ -receptors and cAMP-dependent stimulation of PKA and EPAC2, acts by mobilizing  $Ca^{2+}$  from intracellular stores. We tested for the capacity of adrenaline to induce glucagon secretion and increase  $[Ca^{2+}]_i$  in the presence of

inhibitors of InsP<sub>3</sub> receptor (xestospongin C (32)), sarco/endoplasmic reticulum (sER) Ca<sup>2+</sup> ATPase (thapsigargin or CPA) and Ca<sup>2+</sup>-induced Ca<sup>2+</sup>-release (CICR; ryanodine). Ryanodine, xestospongin C and thapsigargin all inhibited the stimulatory effect of adrenaline on glucagon secretion (Figure 4a) but - unexpectedly - did not appear to affect the adrenaline-induced increase in [Ca<sup>2+</sup>]<sub>i</sub> (

Figure S5a). We reasoned that there might be multiple Ca<sup>2+</sup> release mechanisms operating in parallel in the  $\alpha$ -cell, and that Ca<sup>2+</sup> release via any one of them might suffice to saturate the high-affinity Ca<sup>2+</sup> dye Fluo-4 (which has a K<sub>d</sub> for Ca<sup>2+</sup> of 300nM). Indeed, when the response to adrenaline was instead assayed using the low-affinity indicator Fluo-4FF (K<sub>d</sub>=9.7 $\mu$ M), ryanodine as well as CPA produced marked and statistically significant diminution of the [Ca<sup>2+</sup>]<sub>i</sub>-increasing effect (Figure 4b,c).

Prompted by the observations indicating the presence of a ryanodine-independent component in adrenaline-induced Ca<sup>2+</sup> mobilization, we explored the possible involvement of acidic (lysosomal) Ca<sup>2+</sup> stores (10) in this phenomenon. Bafilomycin, an inhibitor of the vacuolar type-H<sup>+</sup> ATPase, abolished the adrenaline effect on [Ca<sup>2+</sup>]<sub>i</sub> in  $\alpha$ -cells (Figure 4d).

Ca<sup>2+</sup> release from lysosomal stores is mediated by activation of Ca<sup>2+</sup>- and Na<sup>+</sup>-permeable (33;34) two-pore channels (TPCs) (10). We analyzed the role of these channels in the adrenaline-induced [Ca<sup>2+</sup>]<sub>i</sub> increase and glucagon secretion by generation of *Tpcn1* or *Tpcn2* knockout mice. The mRNA of both *Tpcn1* and *Tpcn2* is expressed in mouse and human  $\alpha$ -cells (35-37). Whilst adrenaline increased [Ca<sup>2+</sup>]<sub>i</sub> in  $\alpha$ -cells in islets isolated from *Tpcn1*<sup>-/-</sup> mice (Figure 5a,d), it had very little effect in islets from *Tpcn2*<sup>-/-</sup> mice (Figure 5b, d). The effects of ablating TPC1 and TPC2 on [Ca<sup>2+</sup>]<sub>i</sub> correlated with those on glucagon secretion: adrenaline retained a stimulatory effect on glucagon secretion in *Tpcn1*<sup>-/-</sup> but not *Tpcn2*<sup>-/-</sup> islets (Figure 5c). The effect of adrenaline was seemingly smaller in *Tpcn1*<sup>-/-</sup> than in wild-type islets (but this difference did not attain statistical significance). Ryanodine had no inhibitory effect on glucagon secretion in *Tpcn2*<sup>-/-</sup> islets (Figure 5c). Likewise, pharmacological inhibition of NAADP (the intracellular messenger mobilizing lysosomal Ca<sup>2+</sup> via TPC2 channels) (38;39), which inhibited glucagon secretion in wild-type islets, had no effect in *Tpcn2*<sup>-/-</sup> islets. Genetic ablation ADP-Ribosyl Cyclase 1

(CD38), the enzyme producing NAADP, significantly reduced the increase in  $[Ca^{2+}]_i$  produced by adrenaline (Figure 4d and Figure 5b) and abolished adrenaline-induced glucagon secretion (Figure 5c).

Finally, we tested the effects of culturing islets at 30mM glucose for 72h (as an experimental paradigm of poorly controlled diabetes) on adrenaline's capacity to elevate  $[Ca^{2+}]_i$  and stimulate glucagon secretion. 'Hyperglycemia' abolished the stimulatory action of adrenaline on both  $[Ca^{2+}]_i$  and glucagon secretion (Figure 6a-b,e). By contrast, islets cultured at 11mM glucose (close to the fed plasma glucose levels in mice) responded robustly to adrenaline with both a  $[Ca^{2+}]_i$  increase and stimulation of glucagon secretion. 'Hyperglycemia' did not affect the responsiveness to glutamate (not shown) or effects of adrenaline on  $[cAMP]_i$  and PKA activity (Figure 6c,d).

## Discussion

Adrenaline-induced glucagon secretion involves both PKA- and EPAC2-dependent mechanisms (5). Here we have explored the downstream mechanisms with a focus on intracellular  $Ca^{2+}$  dynamics. Our data are suggestive of a hierarchy of intracellular  $Ca^{2+}$  signaling events and highlight a decisive role of lysosomal stores and NAADP-activated  $Ca^{2+}$  release via TPC2 channels.

Pharmacological inhibition of EPAC2 nearly abolished the stimulatory effect of adrenaline on both glucagon secretion and  $[Ca^{2+}]_i$ . By contrast, inhibition of PKA, whilst lowering  $[Ca^{2+}]_i$  as strongly as inhibition of EPAC2, had only a moderate effect on glucagon secretion. This suggests that a full response to adrenaline requires the activation of *both* PKA-dependent and -independent mechanisms and that EPAC2 may act downstream of PKA (Figure 3c,d).

Given the weak effect of adrenaline on  $\alpha$ -cell electrical activity, the high sensitivity of both adrenaline-induced glucagon secretion and  $[Ca^{2+}]_i$  increase after inhibition of L-type  $Ca^{2+}$  channels may seem paradoxical. However, this effect may be secondary to depletion of intracellular  $Ca^{2+}$  stores when  $Ca^{2+}$  entry is blocked. Indeed, adrenaline retained most of its effect on  $[Ca^{2+}]_i$  when isradipine was added just before adrenaline (Figure 2b).

The mechanism by which adrenaline increases  $[Ca^{2+}]_i$  in  $\alpha$ -cells has variably been attributed to increased  $Ca^{2+}$  channel activity (8) or activation of  $\alpha_1$ -adrenoreceptors (6). Our study unveils a previously unrecognized role of acidic  $Ca^{2+}$  stores in regulation of glucagon secretion.  $Ca^{2+}$  liberated by adrenaline-induced PKA and EPAC2 signaling from the acidic stores then triggers further  $Ca^{2+}$  increase by activating ryanodine-sensitive CICR (40). This hierarchy of intracellular  $[Ca^{2+}]_i$  signaling is supported by the fact that ryanodine exerts no additive inhibitory effect on glucagon secretion in *Tpc2* knockout islets.

Our data suggest a link between PKA/EPAC2 signaling and the *Tpc2* channel activity and the NAADP antagonist Ned19 had no additive inhibitory effect on the adrenaline-induced  $[Ca^{2+}]_i$  increase when PKA and EPAC2 activity was pharmacologically suppressed (Figure 4d). The production of NAADP is influenced by *high* concentrations of cAMP, as expected for an effect mediated by low-affinity cAMP sensor EPAC2 and PKA-dependent phosphorylation of S66 in *Tpc2* increases the channel's open probability (41). The involvement of NAADP production is also illustrated by the ability of the genetic knockdown of the NAADP-generating enzyme CD38 to prevent the effects of adrenaline on both  $[Ca^{2+}]_i$  and glucagon secretion. NAADP-dependent adrenaline-induced  $Ca^{2+}$  release via *Tpc2* channels was recently implicated in the transduction of  $\beta$ -adrenergic signals in cardiomyocytes (42) but not pancreatic  $\beta$ -cells (43;44). The observation that *Tpcn2*<sup>-/-</sup> mice have normal fasting blood glucose (43) it not in conflict with the idea that adrenaline stimulates glucagon secretion by a TPC2-dependent mechanism as adrenaline itself will stimulate hepatic glucose production even in the absence of glucagon and low glucose also stimulates glucagon secretion by a direct (intrinsic) mechanism independent of systemic signals (20;45).

The innervation of mouse and human islets is rather different (46). The finding that adrenaline's effects on  $[Ca^{2+}]_i$  are essentially the same in mouse and human  $\alpha$ -cells may seem at odds with the observation that adrenaline is without effect on glucagon secretion in human islets (23). It is likely that adrenaline produces a transient stimulation of glucagon secretion that escapes detection during a 1h

incubation in human islets. We can exclude though that this discrepancy stems from different glucose concentrations used for secretion measurements (1 mM) and  $[Ca^{2+}]_i$  imaging (3 mM). In a series of initial experiments, adrenaline also increased  $[Ca^{2+}]_i$  in human islets exposed to 1mM glucose (Figure S1a).

Circulating levels of adrenaline are below 1nM, and they remain below 100nM even during exercise (47). Interestingly, these low concentrations of adrenaline inhibit glucagon secretion whilst the stimulatory effect becomes detectable at concentrations  $>1\mu M$  and depends on activation of EPAC2 (5). Such high levels of agonist are unlikely to occur anywhere except close to nerve terminals (48). Thus, our data suggest that the sympathetic signal mediated by locally released noradrenaline (Figure 2b) plays a key role in linking the physiological “flight-or-fight” response to the  $\alpha$ -cell glucagon release. The schematic in Figure 7 presents a model for adrenaline signaling in pancreatic  $\alpha$ -cells. Hypoglycemia elevates systemic adrenaline (released from the adrenal glands) and/or triggers a local release of noradrenaline from sympathetic nerve-endings within or adjacent to pancreatic islets. The catecholamine then binds to a  $\beta$ -adrenoreceptor on the  $\alpha$ -cell, resulting in increased cytosolic cAMP levels, which activate PKA (which interacts with Tpc2 channel residing the membrane of the acidic vesicles) and EPAC2 (which facilitates the liberation of NAADP by CD38). The two signals converge into a release of  $Ca^{2+}$  from the acidic stores into the cytosol, which in turn triggers further liberation of  $Ca^{2+}$  from ER. Altogether, this leads to a four-fold stimulation of the glucagon release and, via stimulation of hepatic glucose concentration, rapid restoration of blood glucose levels. This process depends on background electrical activity of the  $\alpha$ -cell and plasmalemmal  $Ca^{2+}$  entry (explaining the effect of isradipine) to refill intracellular  $Ca^{2+}$  stores.

The mechanism underlying the attenuation of the sympathoadrenal response in diabetes remains debated. Diabetes is associated with the loss of sympathetic islet innervation and this may, via reduced glucagon secretion, account for the increased risk of hypoglycemia (49). It is therefore of interest that our *in vitro* model of chronic hyperglycemia lowers the  $\alpha$ -cell’s intrinsic responsiveness to adrenaline

(Fig. 6d) and thus can itself result in the sympathetic islet neuropathy. The exact mechanism remains to be identified but is likely to be downstream of cAMP and activation of PKA, which were both unaffected. Novel therapeutic strategies that bypass the innervation may help to restore normal counter-regulation in diabetic patients.

### **Author Contributions**

AH, AIT, QZ, AGA performed the experiments and analyzed the data. AG, MZ, NCS, DB provided reagents. GAR, PR, AIT, AG and MZ contributed to data interpretation. PR, AIT, AG and GAR wrote the manuscript.

### **Conflict of interest**

Authors declare no conflicts of interest.

### **Acknowledgements**

We thank Dr Jin Zhang (Department of Pharmacology and Molecular Sciences, The Johns Hopkins University School of Medicine, Baltimore, USA) for the gift of AKAR3. Supported by the MRC Program Grant (G0901521). AH is a recipient of a Diabetes UK PhD Studentship. AG, GAR and PR hold Wellcome Trust Senior Investigator Awards (102828, 098424 and 095531). During the initial stages of the project, AIT held an Oxford Biomedical Research Council postdoctoral fellowship. QZ is a Diabetes UK RD Lawrence Fellow. AIT and PR are the guarantors of the study.



## Figure legends

### Figure 1 The stimulatory effect of adrenaline on glucagon secretion is mediated by selective elevation of $[Ca^{2+}]_i$ in pancreatic $\alpha$ -cells

(a) Glucagon secreted from isolated NMRI mouse islets in response to 3mM glucose with/without 5 $\mu$ M adrenaline. #p<0.05 vs the effect of 3 mM glucose alone. (b) Variance of the Fluo4 intensity when the islet was perfused with 3mM glucose  $\pm$  5 $\mu$ M adrenaline or 20mM glucose (as indicated). The brighter cells are those in which  $[Ca^{2+}]_i$  oscillates. The arrow indicates a cell that started spiking after adrenaline had been applied. (c-d) Typical single  $\alpha$ -cell responses to application of 1mM glutamate and 5 $\mu$ M adrenaline recorded in mouse (c; n=29) and human (d; n=55) islets, at 3mM glucose. (e) Representative  $[Ca^{2+}]_i$  timecourse in the populations of  $\alpha$ - (n=21) and non- $\alpha$ -cells (mostly,  $\beta$ -cells, n=75), differentiated by the response to glutamate. The difference in magnitude of the glutamate and the adrenaline effects was not a consistent finding. (f)  $[Ca^{2+}]_i$  changes in  $\alpha$ -cells quantified as pAUC at 3mM glucose  $\pm$  glutamate or adrenaline in mouse (NMRI, C57Bl/6N) and human islets. p<0.05 vs the respective effect observed in NMRI mice (\*) or the effect of the basal (3 mM glucose) in the same recording (#).

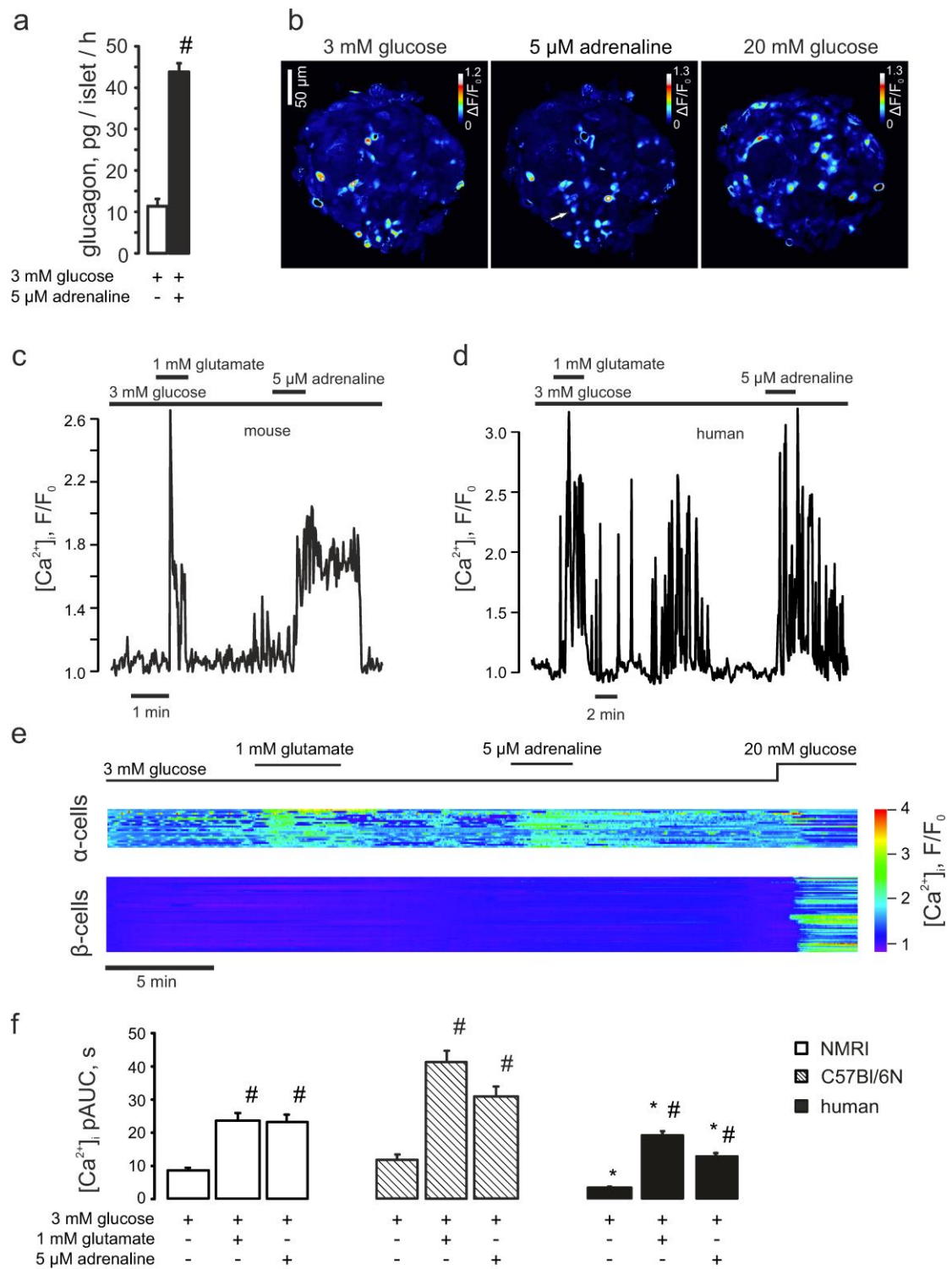


**Figure 2 Adrenaline's effect in pancreatic  $\alpha$ -cells depends on  $\text{Ca}^{2+}$  influx through L-type  $\text{Ca}^{2+}$  channels and is mediated by  $\beta$ -adrenergic signaling**

(a) Glucagon secreted from isolated NMRI mouse islets in response to 3 mM glucose with(out) 5 $\mu$ M adrenaline  $\pm$  isradipine or  $\omega$ -agatoxin (as indicated).  $p < 0.05$  vs the effect of adrenaline + 3mM glucose (\*) or vs the basal (3mM glucose + respective antagonist) group. (b)  $[\text{Ca}^{2+}]_i$  upon adrenergic (isoprenaline (n=27), or noradrenaline (n=19)) stimulation alone (n=29) or with (as indicated) isradipine (n=17, preincubated, n=29, acute),  $\omega$ -agatoxin (n=13), propranolol (n=11), prazosin (n=49), diazoxide (n=20), EGTA (n=84).  $p < 0.05$  vs. the effect of adrenaline alone (\*) or vs the basal (3 mM glucose+respective (ant)agonist) of the same recording. (c) Effect of adrenaline on  $\alpha$ -cell action potential firing (representative of 11 experiments). Examples of action potentials recorded in the absence and presence of adrenaline (taken from the recording above as indicated) are shown.

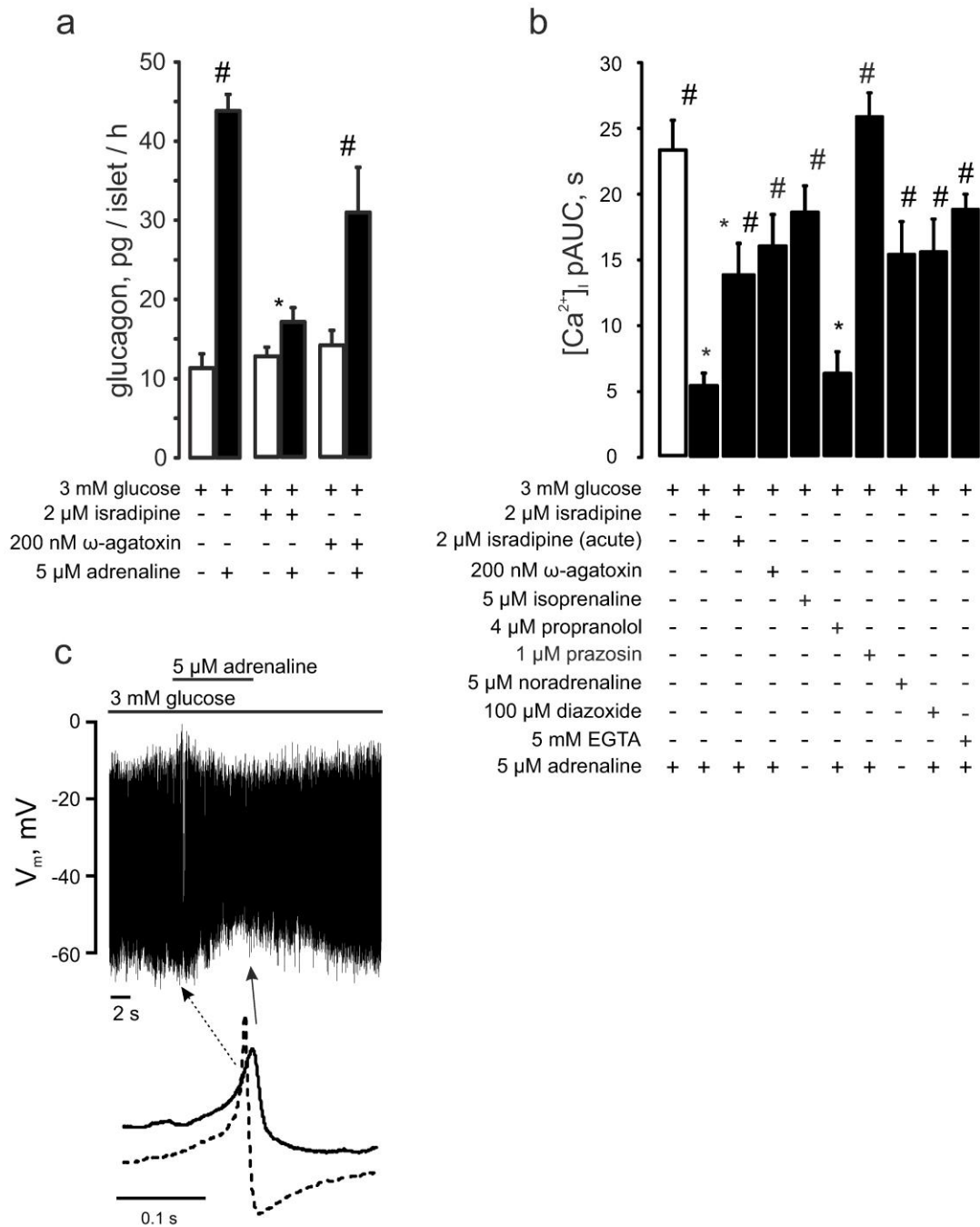


### Figure 3 Adrenaline mediates its effects via elevation of [cAMP]<sub>i</sub>

(a) Glucagon secretion from isolated NMRI mouse islets in response to 3mM glucose. Adrenaline, myr-PKI or ESI-05 was added as indicated.  $p < 0.05$  vs the basal (3 mM glucose + respective antagonist) (#), vs the effect of 3 mM glucose + adrenaline (\*) or vs the effect of 3mM glucose + adrenaline in the presence of ESI-05 (¶). (b)  $[Ca^{2+}]_i$  upon application of (as indicated) adrenaline  $\pm$  myr-PKI (n=32) or ESI-05 (n=12).  $p < 0.05$  vs the basal of the same recording (#) or vs the effect of 3 mM glucose + adrenaline (\*). (c) Representative recording of the depolarization-induced increases in plasma membrane electrical capacitance. (d) Exocytosis in  $\alpha$ -cells. The pipette solution contained (as indicated) either no cAMP (n=7) or 0.1mM cAMP (n=11) and PKA (1 $\mu$ M PKI, n=32) or EPAC2 (25 $\mu$ M ESI-05, n=11).  $p < 0.05$  vs the effect of addition of cAMP into the pipette solution (\*) and vs the control (cAMP-free) condition (#). (e) The effect of adrenaline on PKA activity in  $\alpha$ - (n=22) and  $\beta$ -cells (n=85) within pancreatic islet cells isolated from Glu-RFP mice imaged using AKAR-3 sensor on LSM510 confocal microscope (see also Figure S3 ). The PKA activity is expressed as a change of the FRET ratio of the AKAR-3 sensor. (f) Comparison of the effects of 5 $\mu$ M adrenaline and 1nM-10 $\mu$ M forskolin on PKA activity of pancreatic islet cells (n=870). The excerpt (below, n=62) represents the data from cells activated by adrenaline ( $\alpha$ -cells, see Figure 3e). Note the higher sensitivity of  $\alpha$ -cells to forskolin:  $EC_{50} = 187 \pm 50$  nM (n=24) and  $383 \pm 7$  nM (n=807) for  $\alpha$ - and  $\beta$ -cells, respectively. (g) Representative concentration-PKA activation dependence of  $[Ca^{2+}]_i$  on forskolin in  $\alpha$ -cells measured using Fluo4. (h) Forskolin concentration-activation curves for PKA (solid line, n=98) and  $[Ca^{2+}]_i$  (dashed line, n=20). The effect of 5 $\mu$ M adrenaline on PKA measured on the same cells is mapped on to the curves as a shaded area ( $4.1 \pm 0.8 \mu$ M forskolin).

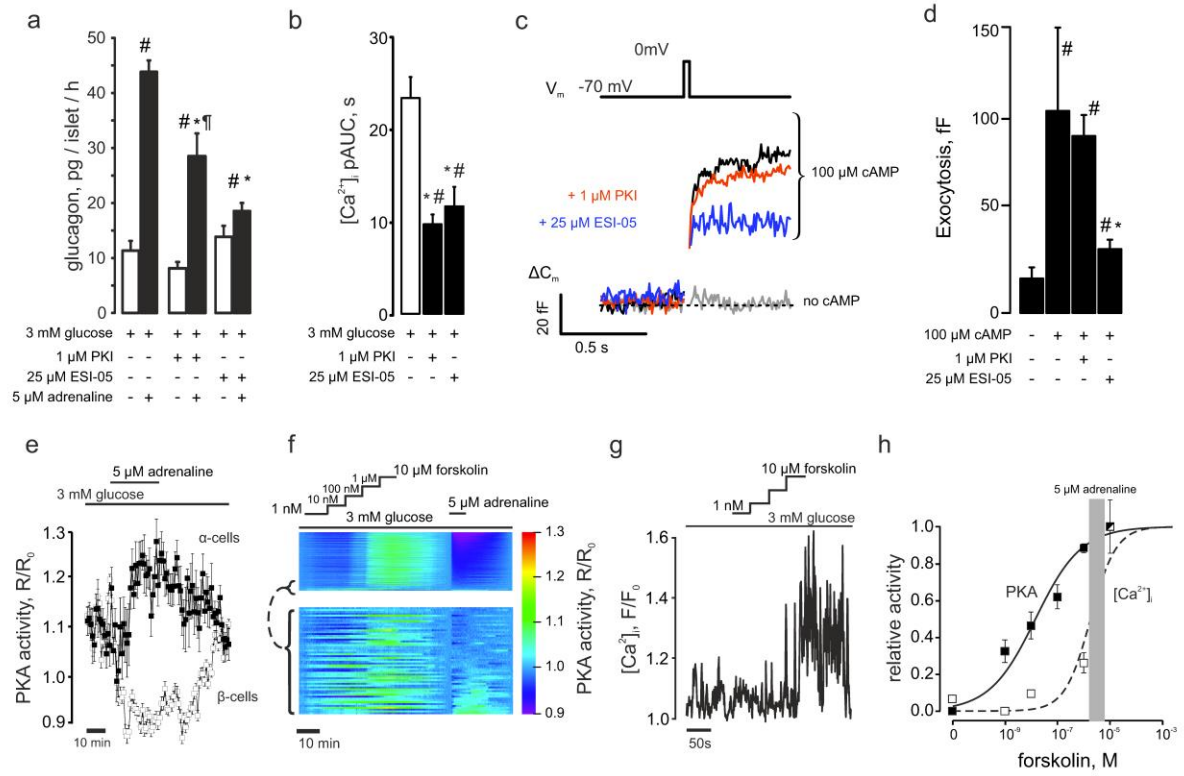


# Figure 4 Adrenaline-induced glucagon secretion involves intracellular $\text{Ca}^{2+}$ release

(a) Glucagon secreted from isolated NMRI mouse islets at 3mM with or without adrenaline and ryanodine, xestospongine C or thapsigargin as indicated.  $p < 0.05$  vs the basal (#) or vs the effect of glucose + adrenaline (\*). (b) Representative recording of the effect of ryanodine on adrenaline-induced  $[\text{Ca}^{2+}]_i$  increases visualized using Fluo4FF. The control (dashed) is superimposed with the experimental trace. (c)  $[\text{Ca}^{2+}]_i$  upon adrenaline stimulation alone (n=23) or in the presence of ryanodine (n=22), xestospongine C (n=30) or CPA (n=14), as measured using Fluo4FF. (d)  $[\text{Ca}^{2+}]_i$  upon adrenaline stimulation alone or in the presence of Ned-19 (n=28), bafilomycin (n=36), myr-PKI and ESI-05 (n=31) or myr-PKI + ESI-05 + Ned-19 (n=21).  $p < 0.05$  vs the basal (3 mM glucose + antagonist) of the same recording (#) or vs the effect of 3 mM glucose + adrenaline (\*). Non-significant ( $p > 0.1$ ) vs the effect of 3mM glucose + adrenaline in the presence of PKI and ESI-05 (§).

Hamilton et al Fig 4

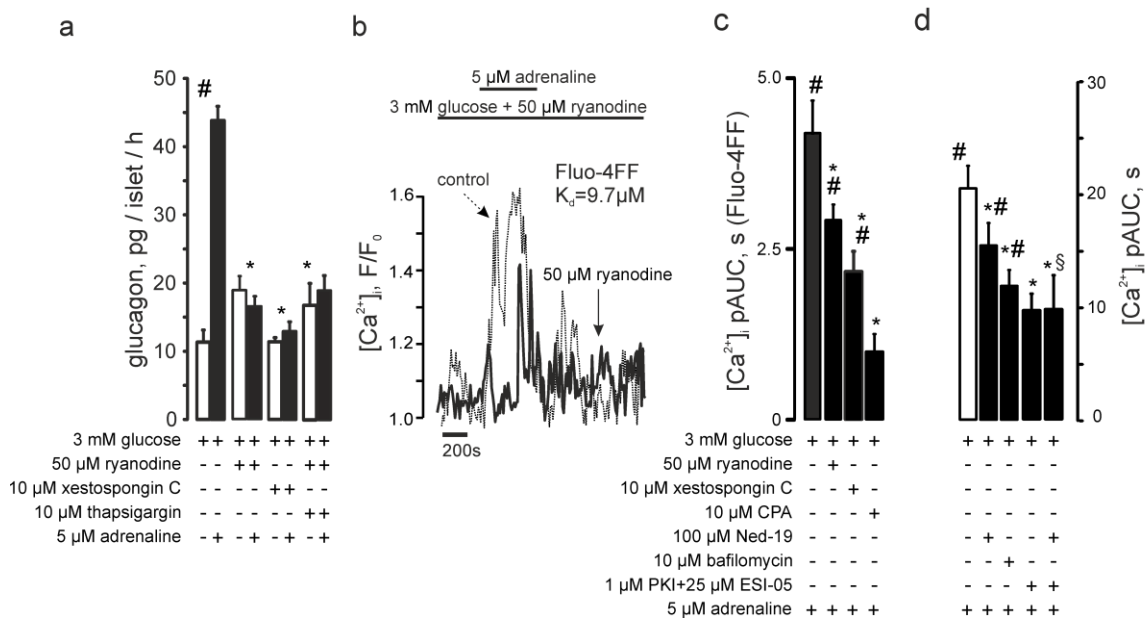


## Figure 5 CD38 and TPC2 but not TPC1 mediate the adrenaline response in $\alpha$ -cells

(a) Effect of adrenaline on  $[Ca^{2+}]_i$  in  $\alpha$ -cells within islets isolated from TPC1<sup>-/-</sup> or TPC2<sup>-/-</sup> mice as indicated. (b)  $[Ca^{2+}]_i$  upon adrenaline stimulation in wild-type, TPC1<sup>-/-</sup> (n=84), TPC2<sup>-/-</sup> (n=27) or CD38<sup>-/-</sup> (n=153) mouse  $\alpha$ -cells.  $p < 0.05$  vs basal (3 mM glucose) of the same recording (#) or vs the effect of 3mM glucose + adrenaline in wild-type animals (§). (c) Glucagon secretion from isolated mouse islets in response to low glucose (3mM) or adrenaline in the absence/presence of Ned-19 or ryanodine, measured in wild-type C57Bl/6n and TPC1<sup>-/-</sup>, TPC2<sup>-/-</sup> and CD38<sup>-/-</sup> mice.  $p < 0.05$  vs the basal (3 mM glucose) (#), vs the effect of 3 mM glucose + adrenaline within the same genotype (\*) or vs the effect of 3mM glucose + adrenaline in wild-type animals (§).

Hamilton et al Fig 5

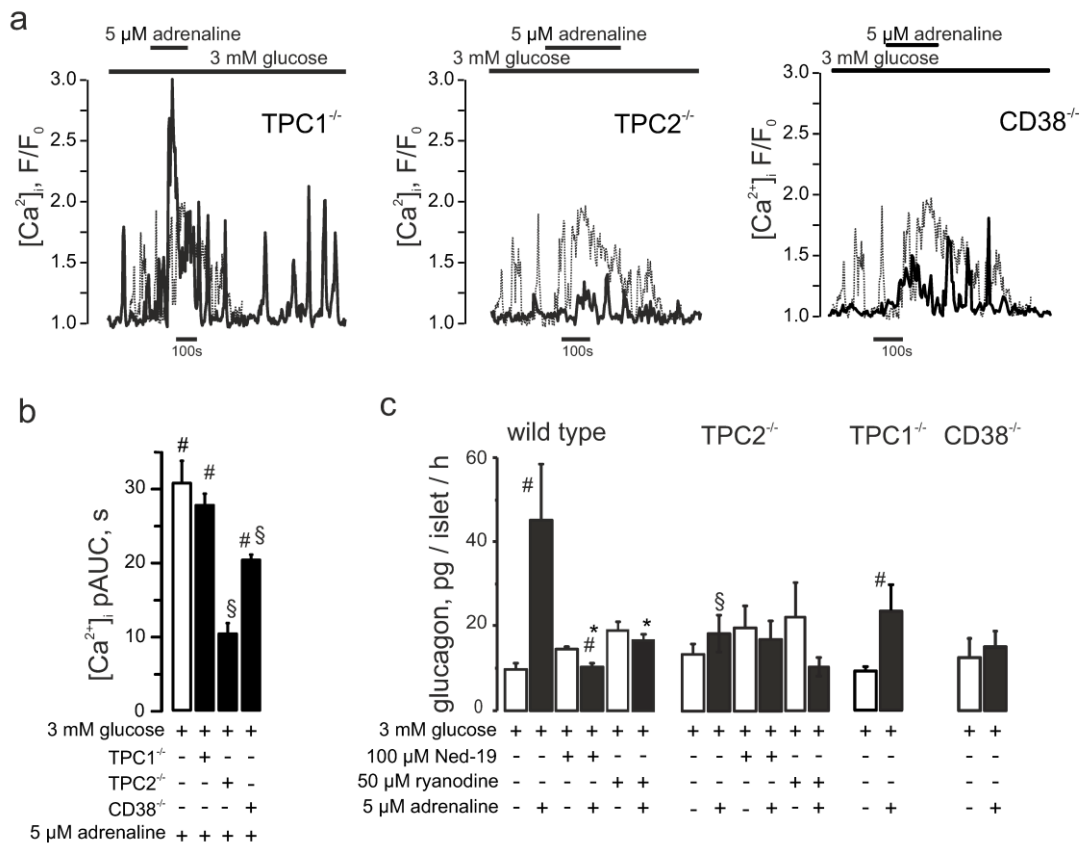




## Figure 6 The adrenaline effect is attenuated by chronic hyperglycemia

(a) Typical  $[Ca^{2+}]_i$  responses to 5  $\mu$ M adrenaline recorded in mouse islet  $\alpha$ -cells precultured at 11 mM (n=102) or 30 mM (n=146) glucose for 48 hours. (b) Quantification of the data presented in (a). p<0.05) vs the basal (3 mM glucose) of the same recording (#) or vs the effect of 3 mM glucose + adrenaline in islets pre-cultured in 11 mM glucose (¶). (c) cAMP responses to adrenaline in pancreatic islet  $\alpha$ -cells pre-cultured at 11 (n=164) or 30mM (n=212) glucose. (d) PKA responses to adrenaline in pancreatic islet  $\alpha$ -cells pre-cultured at 11 (n=1277) or 30 mM (n=1323) glucose. (e) Glucagon secretion from pancreatic islets pre-cultured at 11 (n=10) or 30 mM (n=10) glucose. p<0.05) vs the basal (3 mM glucose) condition (#) or vs the respective effect in islets precultured in 11 mM glucose (¶).

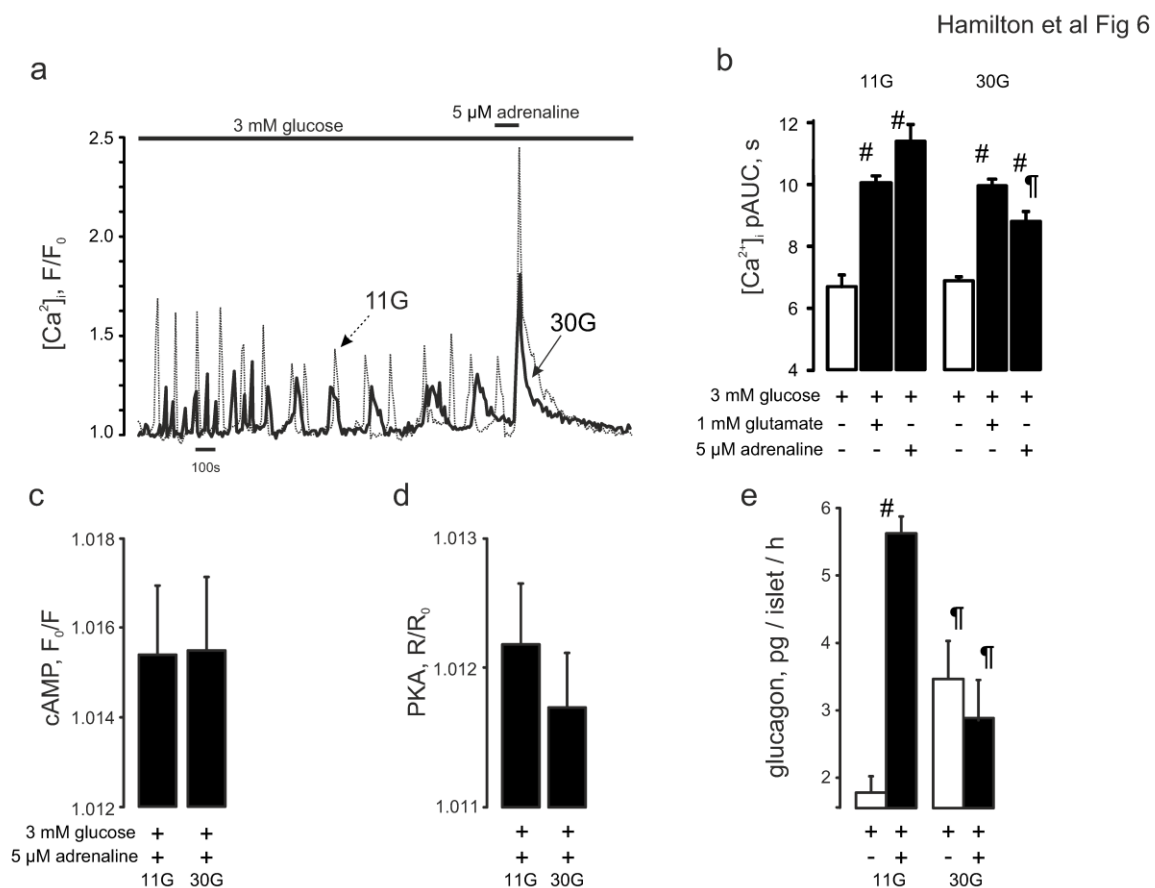
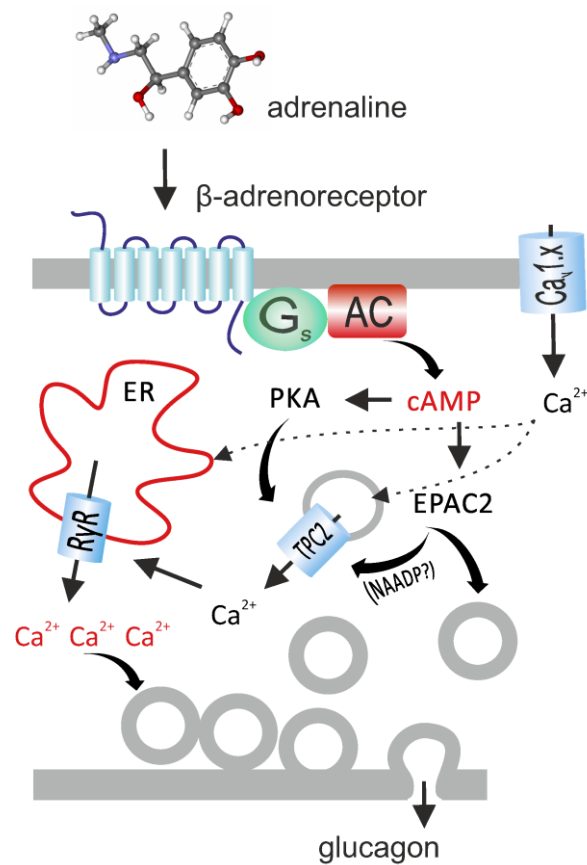


**Figure 7 Model of adrenaline-induced glucagon secretion. See main text for details.**

AC, adenylyl cyclase;  $\text{Ca}_v1.x$ , L-type voltage-gated  $\text{Ca}^{2+}$  channel;  $\text{G}_s$ , G-protein, s  $\alpha$ -subunit. See main text for description.

Hamilton et al Fig7



## References

1. Cryer PE: Hypoglycaemia: the limiting factor in the glycaemic management of Type I and Type II diabetes. *Diabetologia* 2002;45:937-948
2. Gromada J, Franklin I, Wollheim CB: Alpha-cells of the endocrine pancreas: 35 years of research but the enigma remains. *Endocr Rev* 2007;28:84-116
3. Taborsky GJ, Jr., Munding TO: Minireview: The role of the autonomic nervous system in mediating the glucagon response to hypoglycemia. *Endocrinology* 2012;153:1055-1062
4. Skrivarhaug T, Bangstad HJ, Stene LC, Sandvik L, Hanssen KF, Joner G: Long-term mortality in a nationwide cohort of childhood-onset type 1 diabetic patients in Norway. *Diabetologia* 2006;49:298-305
5. De Marinis YZ, Salehi A, Ward CE, Zhang Q, Abdulkader F, Bengtsson M, Braha O, Braun M, Ramracheya R, Amisten S, Habib AM, Moritoh Y, Zhang E, Reimann F, Rosengren AH, Shibasaki T, Gribble F, Renstrom E, Seino S, Eliasson L, Rorsman P: GLP-1 inhibits and adrenaline stimulates glucagon release by differential modulation of N- and L-type  $\text{Ca}^{2+}$  channel-dependent exocytosis. *Cell metabolism* 2010;11:543-553
6. Vieira E, Liu Y-J, Gylfe E: Involvement of  $\alpha_1$  and  $\beta$ -adrenoceptors in adrenaline stimulation of the glucagon-secreting mouse  $\alpha$ -cell. *Naunyn Schmiedeberg's Arch Pharmacol* 2004;369:179-183
7. Johansson H, Gylfe E, Hellman B: Cyclic AMP raises cytoplasmic calcium in pancreatic  $\alpha$  2-cells by mobilizing calcium incorporated in response to glucose. *Cell calcium* 1989;10:205-211
8. Gromada J, Bokvist K, Ding WG, Barg S, Buschard K, Renstrom E, Rorsman P: Adrenaline stimulates glucagon secretion in pancreatic A-cells by increasing the  $\text{Ca}^{2+}$  current and the number of granules close to the L-type  $\text{Ca}^{2+}$  channels. *The Journal of general physiology* 1997;110:217-228
9. Pipeleers DG, Schuit FC, Van Schravendijk CF, Van de Winkel M: Interplay of nutrients and hormones in the regulation of glucagon release. *Endocrinology* 1985;117:817-823
10. Calcra PJ, Ruas M, Pan Z, Cheng X, Arredouani A, Hao X, Tang J, Rietdorf K, Teboul L, Chuang KT, Lin P, Xiao R, Wang C, Zhu Y, Lin Y, Wyatt CN, Parrington J, Ma J, Evans AM, Galione A, Zhu MX: NAADP mobilizes calcium from acidic organelles through two-pore channels. *Nature* 2009;459:596-600
11. Lin WK, Bolton EL, Cortopassi WA, Wang Y, O'Brien F, Maciejewska M, Jacobson MP, Garnham C, Ruas M, Parrington J, Lei M, Sitsapesan R, Galione A, Terrar DA: Synthesis of the  $\text{Ca}^{2+}$ -mobilizing messengers NAADP and cADPR by intracellular CD38 enzyme in the mouse heart: Role in  $\beta$ -adrenoceptor signaling. *The Journal of biological chemistry* 2017;292:13243-13257
12. Lake SP, Bassett PD, Larkins A, Revell J, Walczak K, Chamberlain J, Rumford GM, London NJ, Veitch PS, Bell PR, et al.: Large-scale purification of human islets utilizing discontinuous albumin gradient on IBM 2991 cell separator. *Diabetes* 1989;38 Suppl 1:143-145
13. Ricordi C, Lacy PE, Finke EH, Olack BJ, Scharp DW: Automated method for isolation of human pancreatic islets. *Diabetes* 1988;37:413-420
14. Chen TW, Wardill TJ, Sun Y, Pulver SR, Renninger SL, Baohan A, Schreier ER, Kerr RA, Orger MB, Jayaraman V, Looger LL, Svoboda K, Kim DS: Ultrasensitive fluorescent proteins for imaging neuronal activity. *Nature* 2013;499:295-300
15. Allen MD, Zhang J: Subcellular dynamics of protein kinase A activity visualized by FRET-based reporters. *Biochem Biophys Res Commun* 2006;348:716-721
16. Liu X, Gong H, Li X, Zhou W: Monitoring calcium concentration in neurons with cameleon. *J Biosci Bioeng* 2008;105:106-109
17. Cabrera O, Jacques-Silva MC, Speier S, Yang SN, Kohler M, Fachado A, Vieira E, Zierath JR, Kibbey R, Berman DM, Kenyon NS, Ricordi C, Caicedo A, Berggren PO: Glutamate is a positive autocrine signal for glucagon release. *Cell metabolism* 2008;7:545-554
18. Samols E, Weir GC: Adrenergic modulation of pancreatic A, B, and D cells  $\alpha$ -Adrenergic suppression and  $\beta$ -adrenergic stimulation of somatostatin secretion,  $\alpha$ -adrenergic stimulation of glucagon secretion in the perfused dog pancreas. *J Clin Invest* 1979;63:230-238

19. Panagiotidis G, Salehi AA, Westermark P, Lundquist I: Homologous islet amyloid polypeptide: effects on plasma levels of glucagon, insulin and glucose in the mouse. *Diabetes Res Clin Pract* 1992;18:167-171
20. Zhang Q, Ramracheya R, Lahmann C, Tarasov A, Bengtsson M, Braha O, Braun M, Brereton M, Collins S, Galvanovskis J, Gonzalez A, Groschner LN, Rorsman NJ, Salehi A, Travers ME, Walker JN, Gloyn AL, Gribble F, Johnson PR, Reimann F, Ashcroft FM, Rorsman P: Role of KATP channels in glucose-regulated glucagon secretion and impaired counterregulation in type 2 diabetes. *Cell metabolism* 2013;18:871-882
21. R: A Language and Environment for Statistical Computing [article online], 2016. Available from <https://www.R-project.org/>.
22. Cryer PE: Hypoglycemia, functional brain failure, and brain death. *J Clin Invest* 2007;117:868-870
23. Walker JN, Ramracheya R, Zhang Q, Johnson PR, Braun M, Rorsman P: Regulation of glucagon secretion by glucose: paracrine, intrinsic or both? *Diabetes, obesity & metabolism* 2011;13 Suppl 1:95-105
24. Otter S, Lammert E: Exciting Times for Pancreatic Islets: Glutamate Signaling in Endocrine Cells. *Trends in endocrinology and metabolism: TEM* 2016;27:177-188
25. Rorsman P, Ramracheya R, Rorsman NJ, Zhang Q: ATP-regulated potassium channels and voltage-gated calcium channels in pancreatic alpha and beta cells: similar functions but reciprocal effects on secretion. *Diabetologia* 2014;57:1749-1761
26. Esterhuizen AC, Spriggs TL, Lever JD: Nature of islet-cell innervation in the cat pancreas. *Diabetes* 1968;17:33-36
27. Liu YJ, Vieira E, Gylfe E: A store-operated mechanism determines the activity of the electrically excitable glucagon-secreting pancreatic alpha-cell. *Cell calcium* 2004;35:357-365
28. Wallukat G: The beta-adrenergic receptors. *Herz* 2002;27:683-690
29. Ismail NA, El-Denshary ES, Idahl LA, Lindstrom P, Sehlin J, Taljedal IB: Effects of alpha-adrenoceptor agonists and antagonists on insulin secretion, calcium uptake, and rubidium efflux in mouse pancreatic islets. *Acta Physiol Scand* 1983;118:167-174
30. Hauge-Evans AC, King AJ, Fairhall K, Persaud SJ, Jones PM: A role for islet somatostatin in mediating sympathetic regulation of glucagon secretion. *Islets* 2010;2:341-344
31. Ozaki N, Shibasaki T, Kashima Y, Miki T, Takahashi K, Ueno H, Sunaga Y, Yano H, Matsuura Y, Iwanaga T, Takai Y, Seino S: cAMP-GEFII is a direct target of cAMP in regulated exocytosis. *Nat Cell Biol* 2000;2:805-811
32. Gafni J, Munsch JA, Lam TH, Catlin MC, Costa LG, Molinski TF, Pessah IN: Xestospongins: potent membrane permeable blockers of the inositol 1,4,5-trisphosphate receptor. *Neuron* 1997;19:723-733
33. Ruas M, Davis LC, Chen CC, Morgan AJ, Chuang KT, Walseth TF, Grimm C, Garnham C, Powell T, Platt N, Platt FM, Biel M, Wahl-Schott C, Parrington J, Galione A: Expression of Ca(2)(+)-permeable two-pore channels rescues NAADP signalling in TPC-deficient cells. *The EMBO journal* 2015;34:1743-1758
34. Wang X, Zhang X, Dong XP, Samie M, Li X, Cheng X, Goschka A, Shen D, Zhou Y, Harlow J, Zhu MX, Clapham DE, Ren D, Xu H: TPC proteins are phosphoinositide- activated sodium-selective ion channels in endosomes and lysosomes. *Cell* 2012;151:372-383
35. DiGruccio MR, Mawla AM, Donaldson CJ, Noguchi GM, Vaughan J, Cowing-Zitron C, van der Meulen T, Huising MO: Comprehensive alpha, beta and delta cell transcriptomes reveal that ghrelin selectively activates delta cells and promotes somatostatin release from pancreatic islets. *Mol Metab* 2016;5:449-458
36. Adriaenssens AE, Svendsen B, Lam BY, Yeo GS, Holst JJ, Reimann F, Gribble FM: Transcriptomic profiling of pancreatic alpha, beta and delta cell populations identifies delta cells as a principal target for ghrelin in mouse islets. *Diabetologia* 2016;59:2156-2165
37. Blodgett DM, Nowosielska A, Afik S, Pechhold S, Cura AJ, Kennedy NJ, Kim S, Kucukural A, Davis RJ, Kent SC, Greiner DL, Garber MG, Harlan DM, dilorio P: Novel Observations From Next-Generation RNA Sequencing of Highly Purified Human Adult and Fetal Islet Cell Subsets. *Diabetes* 2015;64:3172-3181

38. Naylor E, Arredouani A, Vasudevan SR, Lewis AM, Parkesh R, Mizote A, Rosen D, Thomas JM, Izumi M, Ganesan A, Galione A, Churchill GC: Identification of a chemical probe for NAADP by virtual screening. *Nat Chem Biol* 2009;5:220-226
39. Galione A: A primer of NAADP-mediated  $\text{Ca}^{2+}$  signalling: From sea urchin eggs to mammalian cells. *Cell calcium* 2015;58:27-47
40. Cancela JM, Churchill GC, Galione A: Coordination of agonist-induced  $\text{Ca}^{2+}$ -signalling patterns by NAADP in pancreatic acinar cells. *Nature* 1999;398:74-76
41. Lee CS-K, Tong BC-K, Cheng CW-H, Hung HC-H, Cheung K-H: Characterization of Two-Pore Channel 2 by Nuclear Membrane Electrophysiology. *Sci Rep* 2016;6:20282
42. Capel RA, Bolton EL, Lin WK, Aston D, Wang Y, Liu W, Wang X, Burton RA, Bloor-Young D, Shade KT, Ruas M, Parrington J, Churchill GC, Lei M, Galione A, Terrar DA: Two-pore Channels (TPC2s) and Nicotinic Acid Adenine Dinucleotide Phosphate (NAADP) at Lysosomal-Sarcoplasmic Reticular Junctions Contribute to Acute and Chronic beta-Adrenoceptor Signaling in the Heart. *The Journal of biological chemistry* 2015;290:30087-30098
43. Arredouani A, Ruas M, Collins SC, Parkesh R, Clough F, Pillinger T, Coltart G, Rietdorf K, Royle A, Johnson P, Braun M, Zhang Q, Sones W, Shimomura K, Morgan AJ, Lewis AM, Chuang KT, Tunn R, Gadea J, Teboul L, Heister PM, Tynan PW, Bellomo EA, Rutter GA, Rorsman P, Churchill GC, Parrington J, Galione A: Nicotinic Acid Adenine Dinucleotide Phosphate (NAADP) and Endolysosomal Two-pore Channels Modulate Membrane Excitability and Stimulus-Secretion Coupling in Mouse Pancreatic beta Cells. *The Journal of biological chemistry* 2015;290:21376-21392
44. Cane MC, Parrington J, Rorsman P, Galione A, Rutter GA: The two pore channel TPC2 is dispensable in pancreatic beta-cells for normal  $\text{Ca}^{2+}$  dynamics and insulin secretion. *Cell calcium* 2016;59:32-40
45. Vieira E, Salehi A, Gylfe E: Glucose inhibits glucagon secretion by a direct effect on mouse pancreatic alpha cells. *Diabetologia* 2007;50:370-379
46. Rodriguez-Diaz R, Abdulreda MH, Formoso AL, Gans I, Ricordi C, Berggren PO, Caicedo A: Innervation patterns of autonomic axons in the human endocrine pancreas. *Cell metabolism* 2011;14:45-54
47. Stich V, de Glisezinski I, Crampes F, Suljkovicova H, Galitzky J, Riviere D, Hejnova J, Lafontan M, Berlan M: Activation of antilipolytic  $\alpha(2)$ -adrenergic receptors by epinephrine during exercise in human adipose tissue. *Am J Physiol* 1999;277:R1076-1083
48. Ludwig J, Gerlich M, Halbrügge T, Graefe KH: The synaptic noradrenaline concentration in humans as estimated from simultaneous measurements of plasma noradrenaline and dihydroxyphenylglycol (DOPEG). *J Neural Transm Suppl* 1990;32:441-445
49. Munding TO, Taborsky GJ, Jr.: Early sympathetic islet neuropathy in autoimmune diabetes: lessons learned and opportunities for investigation. *Diabetologia* 2016;59:2058-2067

## Online Supplemental material

### Supplementary figure legends

#### Figure S1 Partial area under the curve

**(a)** Representative  $[Ca^{2+}]_i$  timecourse in  $\alpha$ -cells (*above*) the populations of islet cells (*below*) showing the effect of the addition of adrenaline at 1 or 3 mM glucose. **(b-c)** Representative  $[Ca^{2+}]_i$  timecourse in the populations of: **(b)** glutamate/adrenaline responsive cells ( $\alpha$ -cells) and  $\delta$ -cells, as differentiated by glutamate response and expression of RFP, respectively, and **(c)**  $\beta$ -cells and  $\delta$ -cells, in sst-RFP mice expressing GCamp3 ubiquitously. **(d)** Representative recording of  $[Ca^{2+}]_i$  dynamics processed and quantified as partial area under the curve (pAUC). The recording (*above*, red) is split into equal time intervals (as indicated by the dashed lines) and area under the curve is computed for each interval (blue). Note that pAUC is sensitive to changes in both  $Ca^{2+}$  frequency and amplitude changes (*below*). **(e)** Representative  $[Ca^{2+}]_i$  timecourse in human  $\alpha$ -cells showing the effect of the addition of adrenaline at 1mM glucose. **(f)** 3-D plot of  $[Ca^{2+}]_i$  (pAUC) values recorded for each individual mouse  $\alpha$ -cell in response to 3mM glucose alone or with glutamate or adrenaline, as indicated. The ideal correlation would assume that the individual cell values are positioned along the main diagonal of the “3 mM glucose”-“glutamate”-“adrenaline” cube.



fig S1

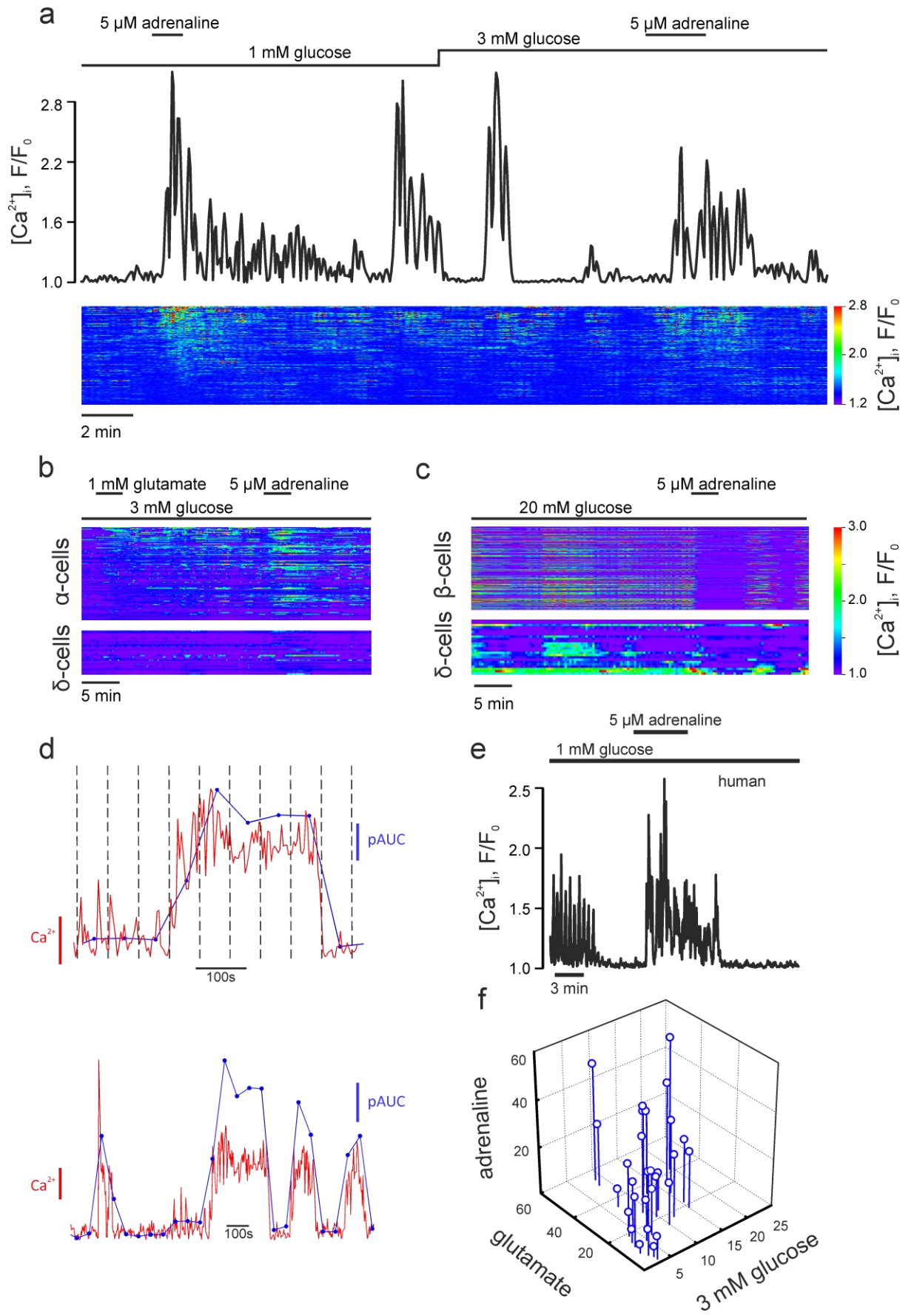




## Figure S2 Stimulatory effect of adrenaline can be dissociated from $\alpha$ -cell electrical activity

**(a)** Action potentials recorded from  $\alpha$ - and  $\delta$  -cells. Note that action potentials in  $\delta$ -cells are much shorter than those in  $\alpha$ -cells and that they are of much larger amplitude. Note that action potentials in  $\delta$ -cells are fired at lower frequency than those in  $\alpha$ -cells and that they are of much larger amplitude. The data was obtained from mouse islets, in which RFP was expressed under tissue-specific promoters to mark  $\alpha$ -cells or  $\delta$ -cells, respectively. **(b-d)** Representative trace of the effect of the acute inhibition of L-type  $\text{Ca}^{2+}$  channels with isradipine **(b)**, chelation of the extracellular  $\text{Ca}^{2+}$  with EGTA **(c)** or opening of  $\text{K}^{+}$  channels with diazoxide on the adrenaline response in the  $\alpha$ -cell. **(e)** Quantification of the effect in **(c, d)**,  $n=84$ ,  $n=72$ , respectively.  $p<0.05$ ) differences vs the effect of 3 mM glucose alone (**¶**) or basal (3 mM glucose+(ant)agonist) of the same recording (**#**). **(f-g)** Effect of isoprenaline on  $\alpha$ -cell action potential frequency (**f**, above) and most negative interspike membrane potential (**f**, below; solid circles) and peak of the spike (**f**, below: open circles) ( $n=11$ ). **(g)** Spike duration ( $n=3$  recordings) in the absence and presence of adrenaline.  $p<0.05$  differences vs effect of 3 mM glucose alone in the same recording (**#**).

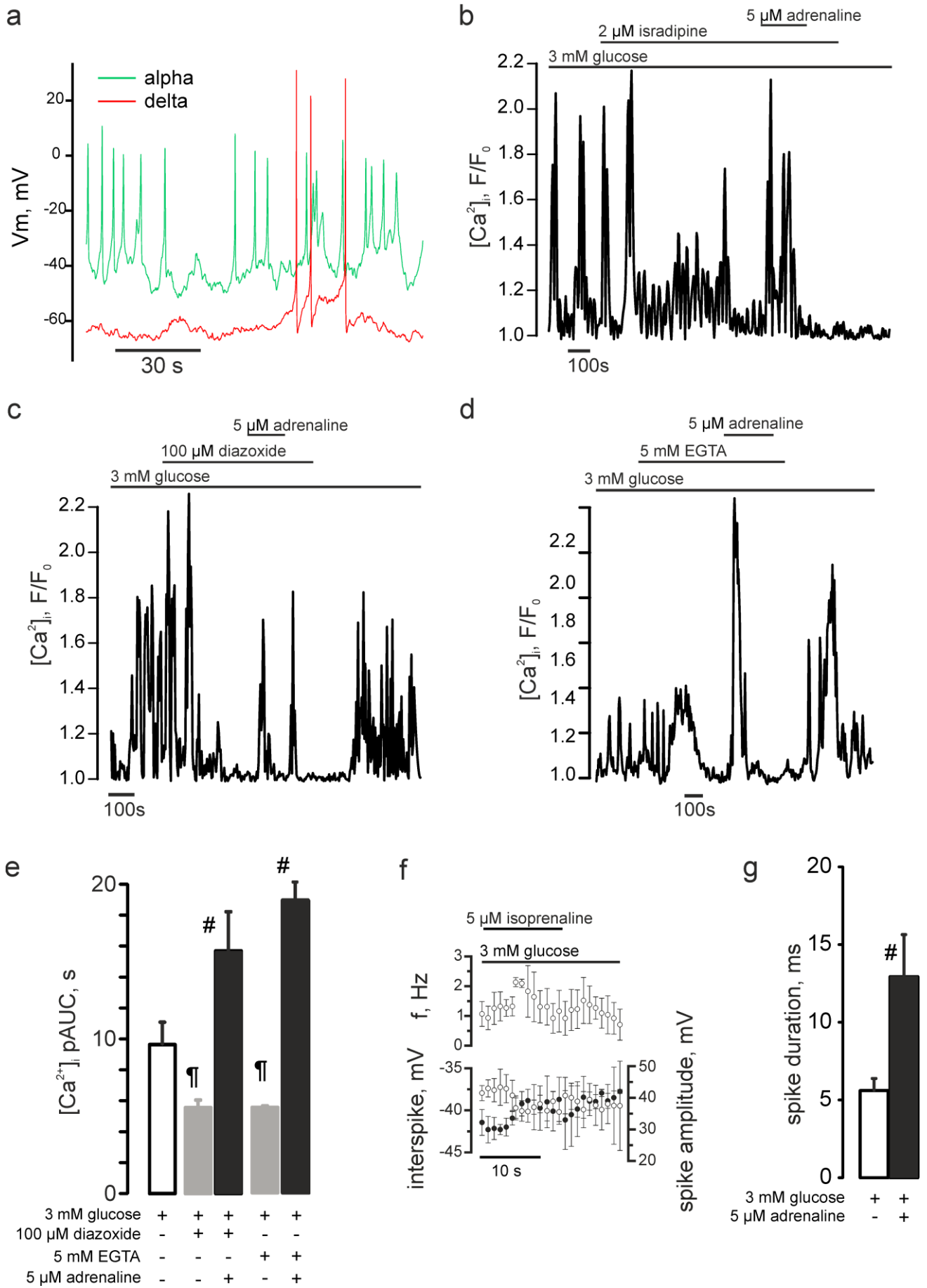
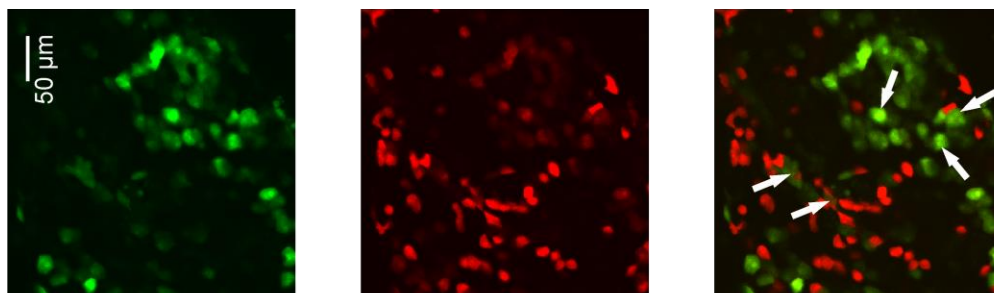


### Figure S3 Adrenaline induces PKA increase specifically in pancreatic $\alpha$ -cells

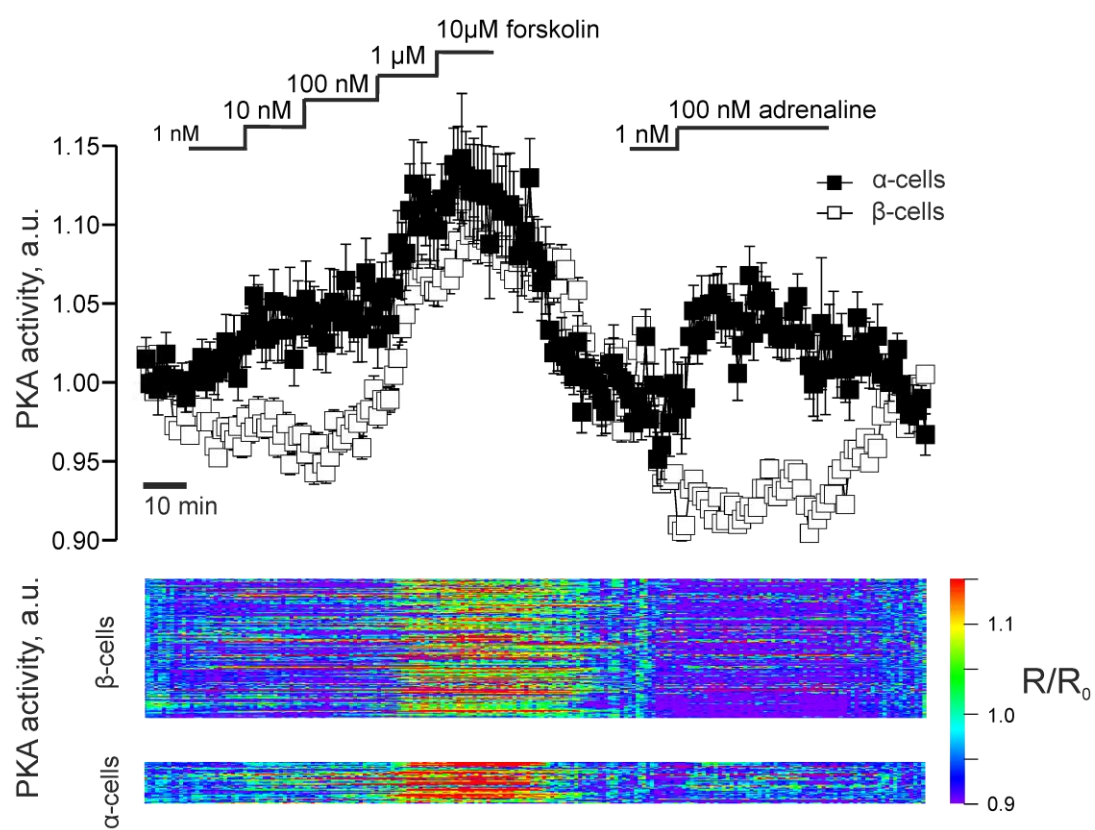
**(a)** Confocal images of Glu-RFP mouse islets expressing AKAR3 sensor; arrows indicate  $\alpha$ -cells expressing AKAR3. **(b)** Changes in PKA activity (quantified as a fold increase of the AKAR3 FRET ratio) in  $\alpha$ - and  $\beta$ -cells in response to forskolin and adrenaline as indicated. The bottom heat map represents the data from all the cells within the islet: each line represents the timecourse of an individual cell, color-coded according to the calibration bar to the right. **(c)** Effect of adrenaline on [cAMP]<sub>i</sub> in human pancreatic islets measured using the downward cADDis sensor and presented as a heat map. Populations of  $\alpha$ -cells (cAMP increases in response to 5 $\mu$ M adrenaline) and  $\beta$ -cells (cAMP decreases in response to 5 $\mu$ M adrenaline) are clearly visible.

fig S3

a



b



c

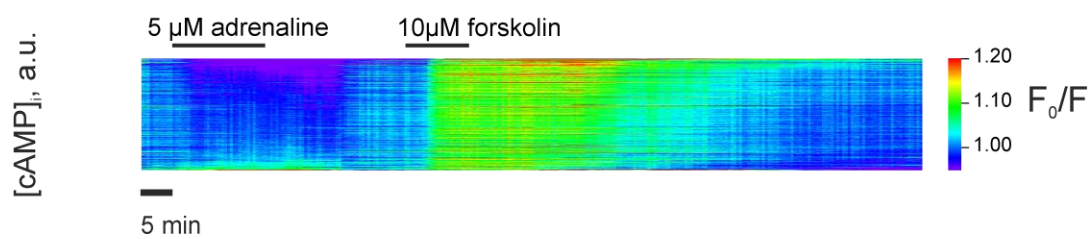


### Figure S4 Effect of pulse duration on capacitance increase

**(a)** Representative traces of capacitance increases in the presence/absence (n=11) of cAMP in the patch pipette, with or without (n=7) myr-PKI (n=32) and ESI-05 (n=11), in response to the 10ms, 20ms, 200ms and 300ms depolarizations. **(b)**  $[Ca^{2+}]_i$  transients evoked by the depolarization steps in (a), imaged simultaneously with cell capacitance measurements. See Figure 3c for responses to a shorter depolarization.

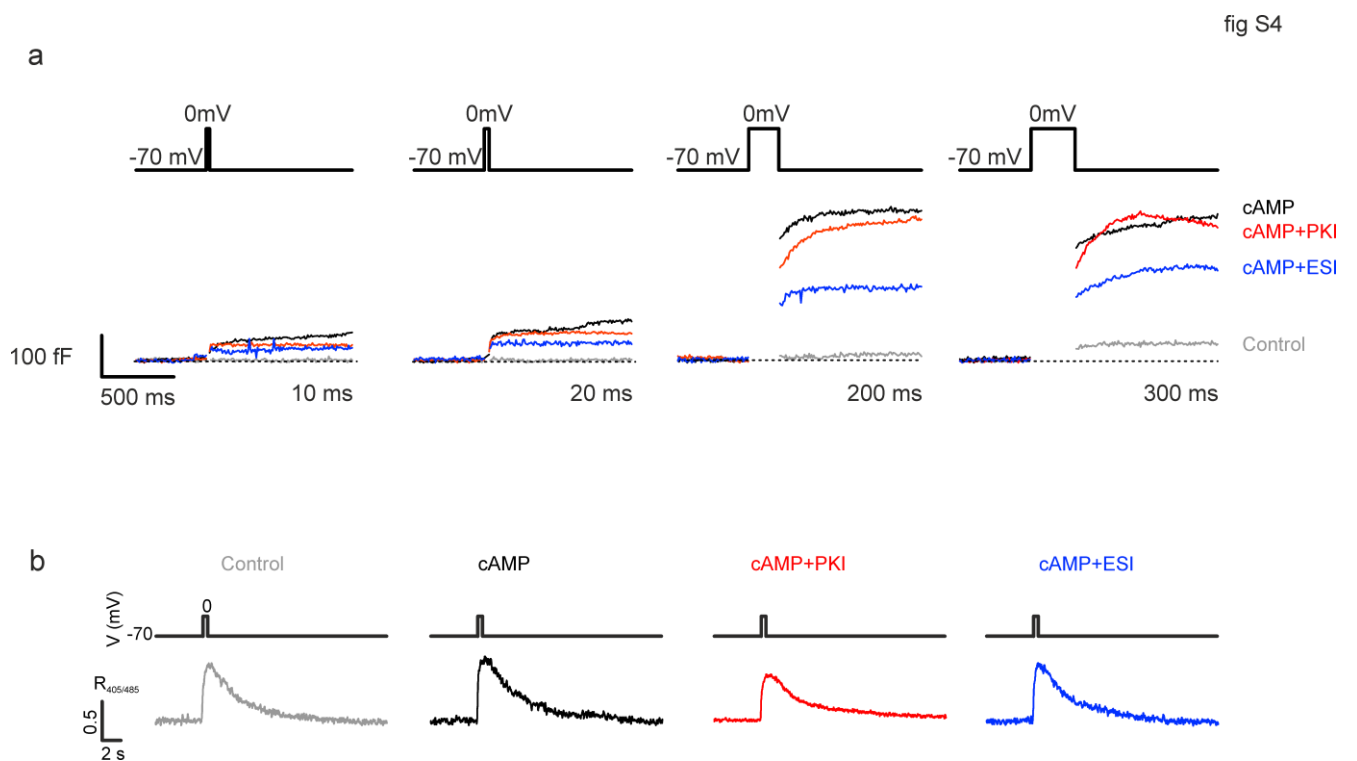
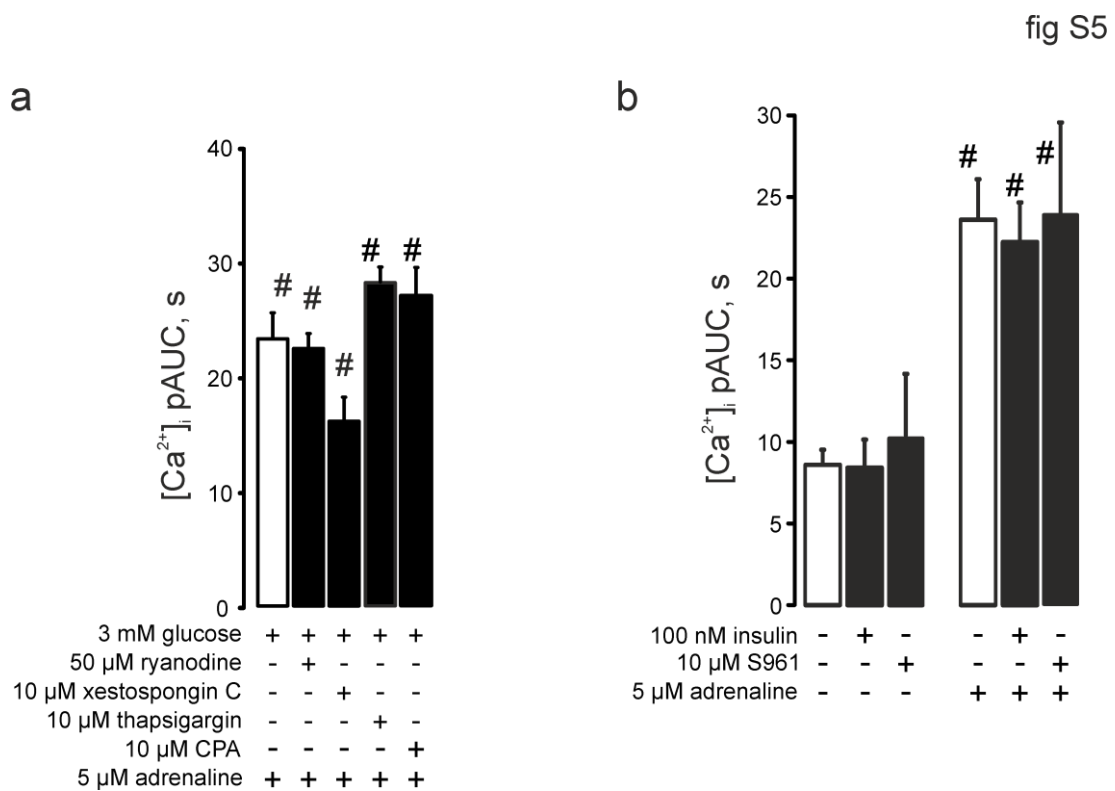


### Figure S5 Role of the $\text{Ca}^{2+}$ release from ER and acute insulin

**(a)**  $[\text{Ca}^{2+}]_i$  quantified as pAUC upon adrenaline stimulation alone or in the presence of ryanodine (n=56), xestospongin C (n=24), thapsigargin (n=23) as indicated. **(b)**  $[\text{Ca}^{2+}]_i$  quantified as pAUC recorded in  $\alpha$ -cells at 3mM glucose with or without 100nM insulin (n=20) or 10  $\mu\text{M}$  S961 (n=20). p<0.05 differences vs the basal (3 mM glucose + antagonist) of the same recording (#).



### **Movie1 Pharmacology of $\text{Ca}^{2+}$ dynamics in pancreatic $\alpha$ -cells**

Timecourse of  $[\text{Ca}^{2+}]_i$  imaged in mouse islet of Langerhans using Fluo-4 dye on the confocal microscope using 40x objective (see Research Design and Methods). The intensity of the dye is coded using a color look-up table, as indicated. Several cells (e.g. the one indicated by the arrow) display clear  $[\text{Ca}^{2+}]_i$  oscillations under basal (3 mM glucose) conditions. Subsequent additions of glutamate and adrenaline dramatically enhance  $\text{Ca}^{2+}$  dynamics in these cells.

[https://www.dropbox.com/s/gdq8pdulwazfyc/Hamilton\\_et\\_al\\_movie\\_01.gif?dl=0](https://www.dropbox.com/s/gdq8pdulwazfyc/Hamilton_et_al_movie_01.gif?dl=0)

### **Movie2 Adrenaline effect interacts with chronic hyperglycemia**

Timecourse of  $[\text{Ca}^{2+}]_i$  imaged in groups of islets precultured at 11 or 30 mM glucose, as indicated, using recombinant sensor GCaMP6f and imaged on a zoom microscope (see Research Design and Methods)

[https://www.dropbox.com/s/dblgi24bmurmc7c/Hamilton\\_et\\_al\\_movie\\_02.gif?dl=0](https://www.dropbox.com/s/dblgi24bmurmc7c/Hamilton_et_al_movie_02.gif?dl=0)